ChemComm

Accepted Manuscript

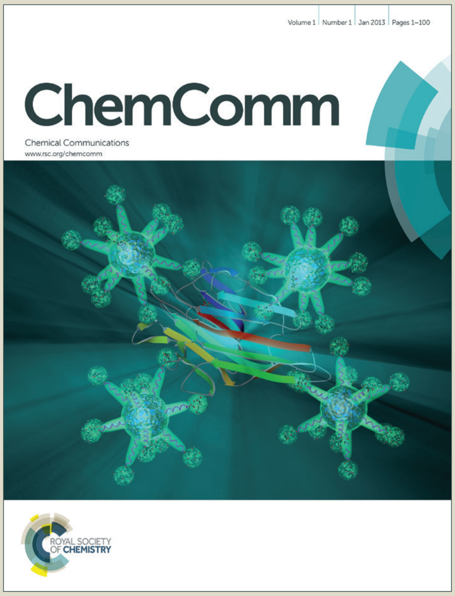

ROYAL SOCIETY OF CHEMISTRY

www.rsc.org/chemcomm

Cite this: DOI: 10.1039/c0xx00000x

www.rsc.org/xxxxxx

ARTICLE TYPE

Beyond Yolk-Shell Nanostructure: A Single Au Nanoparticle Encapsulated in Porous Shell of Polymer Hollow Sphere with Remarkably Improved Catalytic Efficiency and Recyclability

Jie Han*, Minggui Wang, Rong Chen, Na Han, and Rong Guo*

Received (in XXX, XXX) Xth XXXXXXXXX 200X, Accepted Xth XXXXXXXXX 200X
DOI: 10.1039/b000000x

Novel Au-polymer hollow hybrids having a single Au nanoparticle encapsulated in each porous polymer shell with superior catalytic efficiency and recyclability have been demonstrated.

Yolk-shell nanostructured catalysts have been well-established as promising stable and efficient catalysts involved in liquid or gaseous reactions[1-6] due to their structure-related novel properties, where the permeable shells can allow small molecules accessible to active catalytic cores for effective catalytic reaction, meanwhile, prevent coagulation of active catalytic cores.[7, 8] However, the introduction of shells for active catalytic cores will undoubtedly delay the encounter of reaction reagents with catalysts[9, 10] resulting in decreased catalytic efficiency, as compared with bare catalysts without shells. Besides, the crush of yolk-shell catalysts involved in recyclable catalytic reactions and purification processes may cause the release of active catalytic cores and inducing their mutually coagulation.[11] As a result, there is still room for the development of nanocatalysts with improved catalytic efficiency and stability.

In order to improve both the catalytic efficiency and stability for yolk-shell nanocatalysts, it is reasonable to come out the ideal that outward movement of active catalytic cores into porous shells will be the solution. In other words, if active catalytic cores are encapsulated in permeable shells, reagents will be easier to encounter the reactive catalytic cores, leading to increased catalytic efficiency. Moreover, the stability should be enhanced as partial breakage of shells will not release reactive catalytic cores. Therefore, designed-synthesis of hollow structures with active catalytic nanoparticles encapsulated in permeable shells will be more attractive but very challenge.

Herein, we introduce a facile but energetic strategy for the development of polymer hollow nanospheres with a single Au nanoparticle encapsulated in each permeable shell. The schematic illustration for the formation of such novel nanostructured Au-polymer hollow hybrids is given in Figure 1a. Asymmetric Au-polymer core-shell hybrids are firstly synthesized, followed by the swollen treatment in a suitable swelling solvent. Finally, evaporation of swollen Au-polymer core-shell hybrids successfully realizes the solid to hollow nanostructure transformation, where a single Au nanoparticle is encapsulated in each hollow polymer shell.

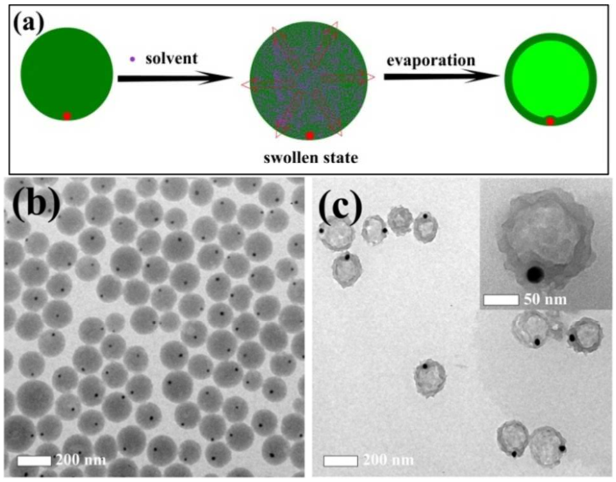

Fig. 1 (a) Schematic illustration for the transformation of asymmetric Au-polymer core-shell hybrids into hollow hybrids with a single Au nanoparticle encapsulated in each polymer shell through swelling-evaporation strategy. (b, c) TEM images of asymmetric Au-POMA core-shell hybrids (b) before and (c) after swelling-evaporation processes.

Poly(*o*-methoxyaniline) (POMA) as a derivative of typical conducting polymer polyaniline with improved swelling performance is chosen for making Au-POMA core-shell hybrids. The original asymmetric Au-POMA core-shell hybrids have been synthesized by the precipitation polymerization of POMA by adding Au colloids (15 nm in average diameter) into the system after the polymerization has proceeded for a few seconds, where the ideal has been firstly proposed for making asymmetric Au-polystyrene core-shell hybrids as reported by Xia et al.[12] Figure 1b shows the original Au-POMA core-shell hybrids with an average size of 200 nm, where essentially every POMA bead contains one Au nanoparticle embedded near the surface. Their excellent uniformity in size and structure has been further confirmed in a low magnified TEM image (Figure S2a) with more than two hundreds particles. Clear observations indicate that Au nanoparticle is not located in the center of each particle, but is quite close to the surface of the POMA bead, confirming their asymmetric core-shell structure (Figure S2b). Then the swelling-evaporation strategy, which can transform polymer particles from solid into hollow nanostructures as developed by us earlier,[13, 14] is applied. When asymmetric Au-POMA core-shell hybrids are treated with a common organic solvent ethanol and then evaporated under ambient conditions, ethanol molecules inside POMA beads, together with POMA polymer chains, move outside, creating void at the center of each POMA bead. Figure 1c shows the typical TEM image of as-synthesized Au-POMA hollow hybrids with one Au nanoparticle encapsulated in each polymer shell, which has been further confirmed in their corresponding SEM image in Figure S3. The average size is similar to their original asymmetric Au-POMA core-shell hybrids, and the POMA shell thickness is about 15 nm, which is close to the size of Au nanoparticle. Clearly observation of the magnified TEM image of one particle as given in inset of Figure 1c proves the inhomogeneity in shell thickness, especially around Au particles shown as prominence inwards. In addition to morphology change, the surface area and average pore size also change upon swelling-evaporation processes. The Brunauer-Emmett-Teller (BET) surface area for Au-POMA core-shell hybrids is 10.5 m^2 g^{-1}, and increases to 50.1 m^2 g^{-1} after swelling-evaporation processes. The average Barret-Joyner-Halenda (BJH) pore diameter calculated from the desorption branch of the isotherm also increases from 4 nm to 11 nm (Figure S4). Therefore, it is believed that in addition to creating voids, the swelling-evaporation processes also loosen the POMA shells.

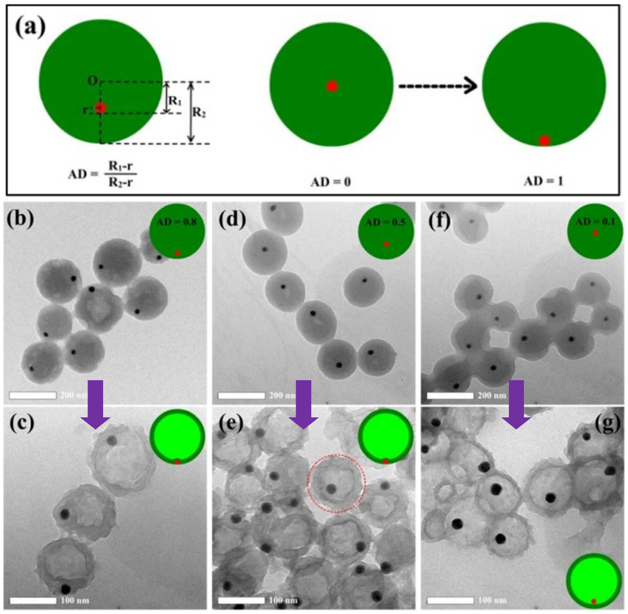

Fig. 2 (a) Schematic illustration for the definition of AD for asymmetric Au-POMA core-shell hybrids. (b-g) TEM images of asymmetric Au-POMA core-shell hybrids (b, d, f) before and (c, e, g) after swelling-evaporation processes with different AD: (b, c) 0.8, (d, e) 0.5 and (f, g) 0.1.

The key factor for realizing the transformation of Au-POMA from core-shell into hollow hybrids with a single Au nanoparticle encapsulated in each POMA shell lies in asymmetry of the original Au-POMA core-shell hybrids. As given in Figure 2a, asymmetry degree (AD) is applied to quantitatively define the eccentricity of Au core in POMA bead with the assumption that AD equals to 0 and 1 means Au core location in center and closely to surface of POMA bead, respectively. Asymmetric Au-POMA core-shell hybrids with different AD have been synthesized by adding Au colloids into POMA polymerization system after the polymerization has proceeded for different times. When addition time of Au colloids is fixed at 60, 50, 10 and 0 s, AD of Au-POMA core-shell hybrids decreases from 1.0 (Figure 1b) to 0.8 (Figure 2b), 0.5 (Figure 2d), and 0.1 (Figure 2f), respectively. After swelling-evaporation processes, Au-POMA hollow hybrids with a single Au nanoparticle encapsulated in each shell of POMA hollow sphere can be found when AD is higher than 0.8 (Figure 1b and Figure 2c). If AD decreases to 0.5, most of the Au cores are encapsulated in shells of polymer hollow spheres, however, there are seldom Au cores locate in hollow interiors shown as yolk-shell nanostructures (Figure 2e and Figure S5). When AD decreases to 0.1 with Au cores mostly located in center of POMA beads, the majority of products show yolk-shell nanostructures (Figure 2g and Figure S6), which agrees well with our previous results.[15] Therefore, it is concluded that Au nanoparticle can be encapsulated in shell of POMA hollow sphere with high AD for asymmetric Au-POMA core-shell hybrids, whereas Au nanoparticle can be located in interiors of POMA hollow sphere under low AD.

Although the formation mechanisms involved in the Au-POMA nanostructure transformation from core-shell to hollow hybrids are not fully understood, the morphological evolution of Au-POMA hollow hybrids with decreasing AD of Au-POMA core-shell hybrids hints that hollowing of POMA beads during evaporation process should start from the center of POMA beads (Figure 1a). Under circumstances of high AD of Au-POMA core-shell hybrids with Au nanoparticles mainly locate near surfaces of POMA beads (Figure 1b, Figure 2b, and Figure 2d), the outward migration of swelling solvent ethanol together with POMA polymer chains should firstly start from center of POMA bead during evaporation process. When ethanol solvents move near polymer surfaces, they are directly evaporated, leaving porous POMA polymers as shells of hollow beads (Figure 1c, Figure 2c, and Figure 2e). However, in region of Au nanoparticle embedded near surface, ethanol should move around due to impermeable nature of Au crystal, and eventually leaving polymer prominences inwards (inset in Figure 1c). Under low AD of Au-POMA core-shell hybrids with Au nanoparticles mainly located in center of POMA beads (Figure 2f), the outward migration of ethanol together with POMA polymer chains during evaporation process should firstly begin around Au nanoparticle-POMA polymer interfaces, and eventually resulting in Au nanoparticle located inside POMA hollow spheres shown as Au-POMA yolk-shell hybrids (Figure 2g).

Moreover, the stability of Au-POMA hollow hybrids with one Au nanoparticle encapsulated in each polymer shell has been considered. It is found that another cycle of swelling-evaporation processes with ethanol as the swelling reagent will not affect their structure. It has been confirmed that POMA shells has been loosen during the first cycle of swelling-evaporation processes. Therefore, solvent molecules will diffuse freely across the porous polymer shell, which leaves less impact on their original structure.

Finally, the catalytic performances of Au-POMA hybrids were evaluated using a model reaction of liquid-phase reduction of 4-nitrophenol (4-NP) to 4-aminophenol (4-AP) in the presence of $NaBH_4$. Time-dependent adsorption spectra of this reaction mixture show the disappearance of the peak at 400 nm that accompanied by a gradual development of a new peak at 300 nm corresponding to the formation of 4-AP (Figure S7). Since excess $NaBH_4$ is present in the reaction solution and the reduction of 4-NP by $NaBH_4$ is negligible in the absence of Au nanoparticles, the reaction can be considered pseudo-first-order with respect to the concentration of 4-NP.[16, 17] Firstly, the catalytic efficiency of Au-POMA core-shell hybrids with lowest and highest AD have been considered. As given in Figure 3a, no measurable catalytic activity could be detected at low AD (0.1, Figure 2f) with Au nanoparticle deeply embedded in polymer beads, whereas the catalytic reaction could be proceeded with the kinetic reaction rate constant (defined as k_{app}) calculated to be 0.045 min^{-1} at highest AD (1.0, Figure 1b) with Au nanoparticle mostly located near surfaces. As for Au nanoparticle without polymer shell, the k_{app} is estimated to be 0.26 min^{-1}, almost six times larger than that of asymmetric Au-POMA core-shell hybrids with highest AD. Although outward of Au nanoparticle in Au-POMA core-shell hybrids facilitates the encounter of reaction reagents with catalytic cores, the catalytic efficiency is still lower than that of pure Au nanoparticles due to the block of dense polymer coating.

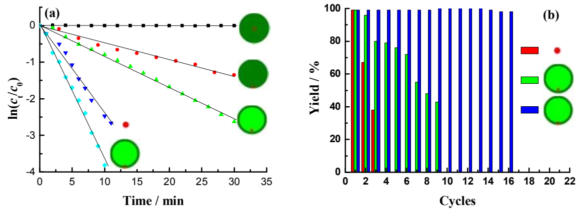

Fig. 3 (a) Plot of $\ln(c_t/c_0)$ of 4-NP against time using different catalysts. (b) Synthesis yield of 4-AP in the successive reactions with different cataysts.

When Au-POMA core-shell hybrids (AD = 0.1) were transformed into Au-POMA yolk-shell hybrids (Figure 2g) through swelling-evaporation processes, the catalytic efficiency was significantly improved with k_{app} of 0.088 min^{-1}, about twice higher than that of Au-POMA core-shell hybrids with AD of 1.0. Although the reactive Au cores are located near surfaces in Au-POMA core-shell hybrids, the dense polymer coating may retard mass transfer and therefore inhibit the catalytic processes, whereas catalytic centers of Au nanoparticles in Au-POMA yolk-shell nanostructures are movable and surrounded by thin and loose polymer shells, which are favorable for mass transfer to catalytic centers. Surprisingly, when using Au-POMA hollow hybrids with Au nanoparticle encapsulated in each polymer shell (Figure 1c) as catalysts, k_{app} is largely improved to 0.38 min^{-1}, even higher than that using pure Au nanoparticles as catalysts. In this case, it is believed that reaction reagents both inside and outside polymer shells can be easily accessible to the reactive centers due to porous polymer shells with large pore size and thin shell thickness with active Au cores close to both surfaces. Besides, the intrinsic conducting nature of POMA favors electron transfer of catalysts due to their effective contact,[18] which is believed to contribute to the improved catalytic efficiency.

Although recyclability is usually regarded as an advantage of heterogeneous catalysts, their practical applications in liquid-phase reactions still suffer from reduced catalytic activity resulting from nanoparticle coagulation.[19, 20] Herein, the recyclability of Au nanoparticles, Au-POMA yolk-shell hybrids, and Au-POMA hollow hybrids with one Au nanoparticle encapsulated in each polymer shell were revealed (Figure 3b). It is found that Au nanoparticles only can be reused three times with apparent decreasing in catalytic efficiency. As for Au-POMA yolk-shell hybrids, they can be survived in nine cycles also with steady decreasing in catalytic efficiency. Interestingly, the catalytic efficiency almost unchanged in at least sixteen cycles using Au-POMA hollow hybrids with Au nanoparticle encapsulated in each polymer shell, which proves their excellent recyclability. It is not surprisingly that pure Au catalysts will lose their catalytic activity after several cycles due to the conglomeration of nanoparticles. As for Au-POMA yolk-shell hybrids, partial aggregation of Au nanoparticles caused by the cracking of polymer shells during centrifugation and purification processes should be accounted for decrease catalytic activity.[15] In respect to Au-POMA hollow hybrids with Au nanoparticle encapsulated in each polymer shell, cracking of polymer shells during centrifugation and purification processes should not lead to release of Au nanoparticle because Au nanoparticles are buried in polymer shells. Instead, detectable increase in catalytic activity has been evidenced during recycling processes (Figure 3b), as the cracking in polymer shells can facilitate the mass transfer.

In conclusion, a novel nanostructured catalyst with a single Au nanoparticle encapsulated in porous shell of polymer hollow sphere has been firstly reported through a facile swelling-evaporation processes originated from asymmetric Au-POMA core-shell hybrids. The high AD of original Au-POMA core-shell hybrids is found to be the key factor in the formation of such novel nanostructure. Their superior catalytic efficiency and recyclability have also been established, indicating their potential applications as efficient and recyclable catalysts involved in liquid-phase catalysis. It is believed that the catalytic core and polymer shell can be extended for preparing robust catalysts for various reactions.

The authors gratefully acknowledge financial support from the National Natural Science Foundation of China (No. 21273004, 20903079 and 21073156) and the Priority Academic Program Development of Jiangsu Higher Education Institutions. We would also like to acknowledge the technical support received at the Testing Center of Yangzhou University.

Notes and references

School of Chemistry and Chemical Engineering, Yangzhou University, Yangzhou, Jiangsu, China. Fax: 86 514 8797 5219; Tel: 86 514 8797 5219; E-mail: hanjie@yzu.edu.cn; guorong@yzu.edu.cn

† Electronic Supplementary Information (ESI) available: Experimental details and additional figures. See DOI: 10.1039/b000000x/

1 S. Kim, Y. Yin, A. P. Alivisatos, G. A. Somorjai and J. T. Yates, *J. Am. Chem. Soc.*, **2007**, *129* , 9510.
2 C. H. Kuo, Y. Tang, L. Y. Chou, B. T. Sneed, C. N. Brodsky, Z. Zhao and C. K. Tsung, *J. Am. Chem. Soc.*, **2012**, *134*, 14345.
3 Y. Yang, X. Liu, X. Li, J. Zhao, S. Bai, J. Liu and Q. Yang, *Angew. Chem., Int. Ed.*, **2012**, *51*, 9164.
4 Y. Chen, H. R. Chen and J. L. Shi, *Acc. Chem. Res.*, **2014**, *47*, 125.
5 J. Liu, H. Q. Yang, F. Kleitz, Z. G. Chen, T. Yang, E. Strounina, G. Q. Lu and S. Z. Qiao, *Adv. Funct. Mater.*, **2012**, *22*, 591-599.
6 S. Wu, J. Dzubiella, J. Kaiser, M. Drechsler, X. H. Guo, M. Ballauff, Y. Lu, *Angew. Chem. Int. Ed.*, **2012**, *51*, 2229.
7 X. J. Wu and D. Xu, *J. Am. Chem. Soc.*, **2009**, *131*, 2774.
8 C. H. Lin, X. Liu, S. H. Wu, K. H. Liu and C. Y. Mou, *J. Phys. Chem. Lett.*, **2011**, *2*, 2984.

9 I. Lee, J. B. Joo, Y. Yin and F. Zaera, *Angew. Chem. Int. Ed.,* **2011**, *50*, 10208.
10 H. Sun, X. Shen, L. Yao, S. Xing, H. Wang, Y. Feng and H. Chen, *J. Am. Chem. Soc.,* **2012**, *134*, 11243
11 P. M. Arnal, M. Comotti and F. Schüth, *Angew. Chem. Int. Ed.,* **2006**, *45*, 8224.
12 A. Ohnuma, E. C. Cho, P. H. C. Camargo, L. Au, B. Ohtani and Y. Xia, *J. Am. Chem. Soc.,* **2009**, *131*, 1352.
13 J. Han, G. Song and R. Guo, *J. Polym. Sci., Part A: Polym. Chem.,* **2007**, *45*, 2638
14 J. Han, L. Wang and R. Guo, *Macromol. Rapid Commun.,* **2011**, *32*, 729
15 J. Han, R. Chen, M. Wang, S. Lu, R. Guo, *Chem. Commun.,* **2013**, *49*, 11566.
16 Q. Zhang, T. Zhang, J. Ge and Y. Yin, *Nano Lett.,* **2008**, *8*, 2867.
17 J. Han, L. Li and R. Guo, *Macromolecules,* **2010**, *43*, 10636.
18 J. Han, M. Wang, S. Cao, P. Fang, S. Lu, R. Chen and R. Guo, *J. Mater. Chem. A,* **2013**, *1*, 13197.
19 Q. Zhang, I. Lee, J. Ge, F. Zaera and Y. Yin, *Adv. Funct. Mater.,* **2010**, *20*, 2201.
20 I. Lee, Q. Zhang, J. Ge, Y. Yin and F. Zaera, *Nano Res.,* **2011**, *4*, 115.